

Dopant-Rich Films on Si:

A new frontier for thermal ALD processes

Michael I. Current, Current Scientific, San Jose, CA

with...

T.E. Seidel, Seitek50, Palm Coast, FL,

J. W. Elam and A. U. Mane, Argonne National Laboratory, Argonne, IL,

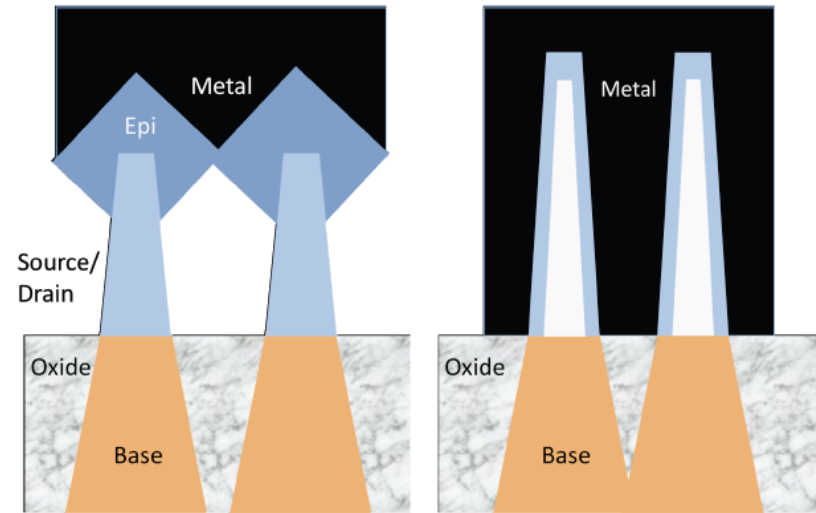
A. Goldberg and M. D. Halls, Schrodinger, Inc., San Diego, CA,

J. Despres, O. Byl, Y. Tang, J. Sweeney, Entegris, Danbury, CT.

1. How to dope 3D structures?: finFETs, V-NAND
2. DFT calculations of B & P on Si
3. B₂F₄ ALD growth kinetics
4. Conformality & thermal drive-in
5. Summary

3D Doping: finFETs (1)

When finFETs shift from epi-top contacts to larger area sidewall metal-Si contacts, fin sidewall doping will need to be (1) much more uniform and (2) higher active concentration.



Near-surface “shell” doping in thin fins can be used for high-performance junctionless channels **IF** the doping is very thin (<2 nm) with high-active concentration.

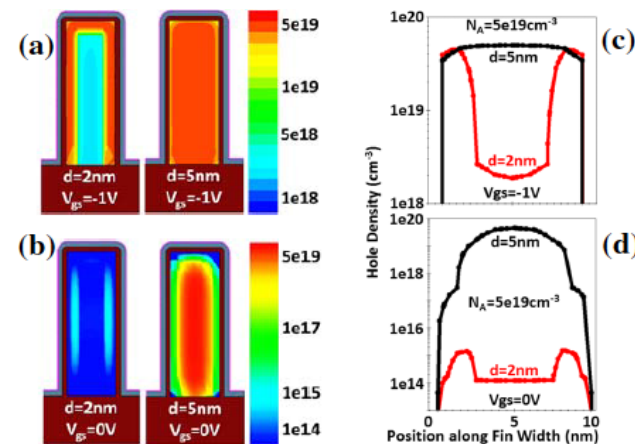


Fig. 4. 2D hole distribution in the fins for $V_{gs} = -1/0$ V (a/b). 1D hole distribution along the fin for $V_{gs} = -1/0$ V (c/d). Note that similar results have been observed in n-channel devices (not shown). ($V_{ds} = -0.5$ V)

T. Seidel et al., “ALD Process for Dopant Rich Films on Si”, IIT16.
Y.J. Lee et al., “Junctionless FET with sub-5nm Shell Doping” IEDM14.

3D Doping: V-NAND (2)

3D-NAND shipping now at 48/64 layers.
96 layer versions due in 2018.
Channel AF >50:1.

How to dope the channels for V_{th} ?

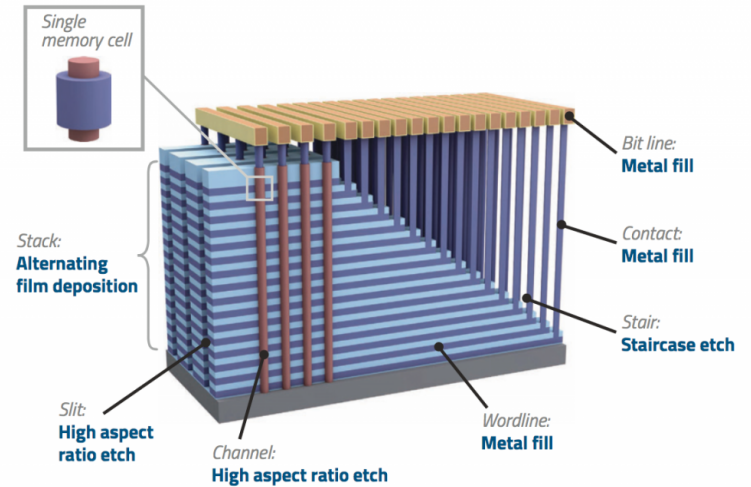


FIGURE 1. 3D NAND architecture showing some of the most challenging and critical deposition and etch processes.

PIII/PLAD doping is good for finFETs and “modest” AR trench/via/channels, but for AR >50 ?

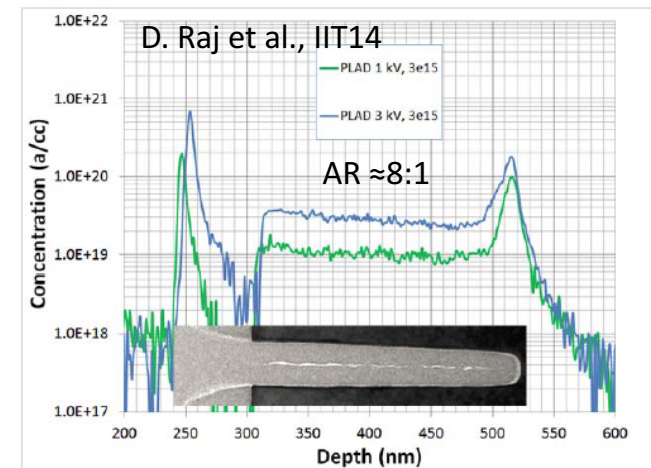


Fig. 3. 3D memory cell structure doping. HAR SIMS data with energy sensitivity at 1 and 3 kV, $3e15$ a/cm².

Recoil Implants (1)

Recoil implants (“ion beam mixing”) have been used for a long time.

Key advantages (for glancing angles) are:

1. recoil dose is much larger ($\approx \times 100$) than the incident ion dose.
2. recoil mixing profile is “shallower” than the incident ions.
3. recoil dose is not very sensitive to either (a) incident ion energy or (b) incident ion angle.
4. implant damage can be limited to (mostly) the surface (source) layer.

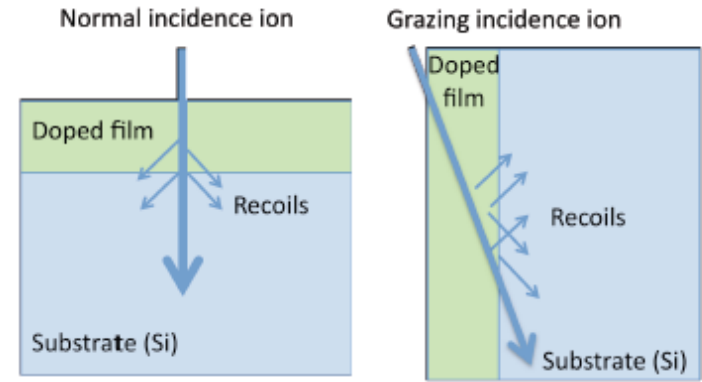


Figure 4. Sketches of recoil mixing for normal and glancing angle incidence ions.

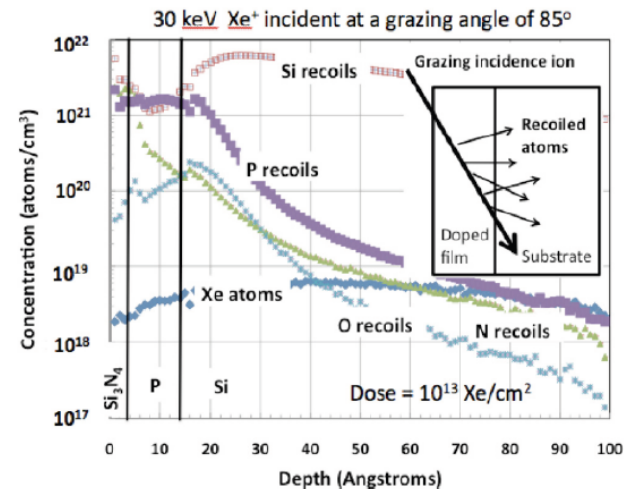


Fig. 8. Calculated recoils and implanted 30 keV Xe for an 85° grazing incident Xe^+ beam on a Si_3N_4 capped, 1 nm thick P layer (with a monolayer SiO_2 interface layer) on Si for a dose of 10^{13} Xe/cm^2 . Note the high concentration of P relative to Xe atoms.

Recoil Implants (2)

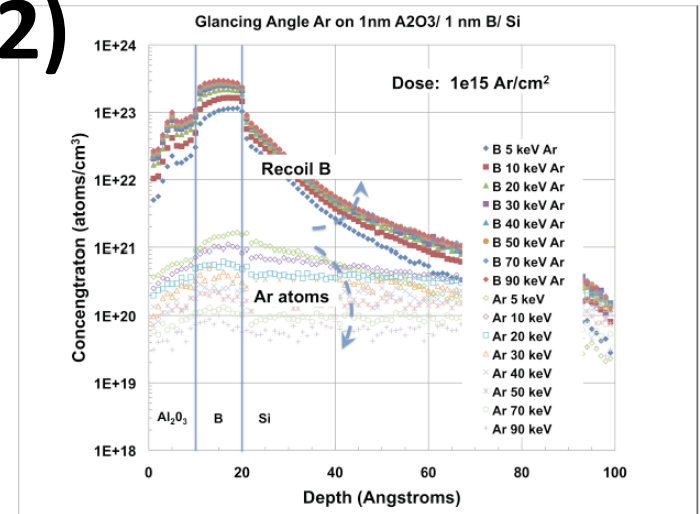


Figure 6. B recoils and implanted Ar for glancing (85°) incidence Ar ions on a 1nm B layer with a 1 nm Al₂O₃ cap for ion energies of 5 to 90 keV. The arrows show the profile trends with increasing Ar energy.

Recoil mixing profiles of B surface films are substantially the same for glancing incidence Ar⁺ ions for > 40 keV.

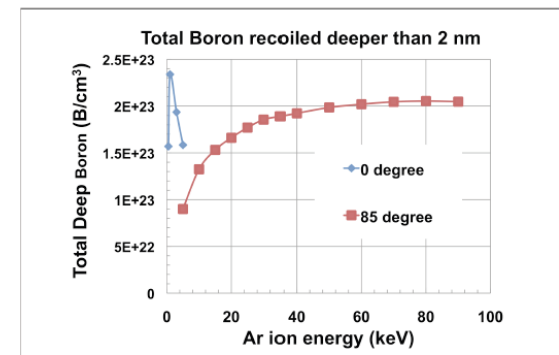


Figure 8. Total recoil B atoms deeper than 2 nm for normal and glancing angle incident Ar beams at a dose of 1e15 Ar/cm². Although the peak B recoil doping levels are similar (note the linear vertical scale), the normal incident case is strongly dependent on Ar energy and limited to low (1 keV) ion energies for these model thin ALD films. The glancing angle B recoil yield is substantially independent of Ar energy above ≈40 keV.

Thermal ALD of Dopants: circa 2014

OK, all we have to do is:

- (1) look up recipes for ALD of thin dopant rich films,
- (2) grow dopant-rich ALD films,
- (3) do recoil implant (or thermal drive in),
- (4) ship devices,
- (5) enjoy a celebratory fine wine.

But, as of Sept 2014, there were **NO PUBLISHED PAPERS** on thermal ALD* of dopant rich films on Si in the ANL database (>2.5k ALD papers)!

So, call your friends who do quantum chemistry calculations.

* There are plenty of papers for thermal deposition, PE CVD/ALD, etc....all with questions on conformality for extreme 3D surfaces.

Density Functional Theory for B & P on Si (1)

By comparison with the “Grand Dad” of ALD applications, W-deposition with WF_6 , initial calculations with PF_3 (using Density Function Theory (DFT) at Schrodinger, Inc.) also looked favorable.

A. Goldberg and M. D. Halls, Schrodinger, Inc., San Diego, CA,

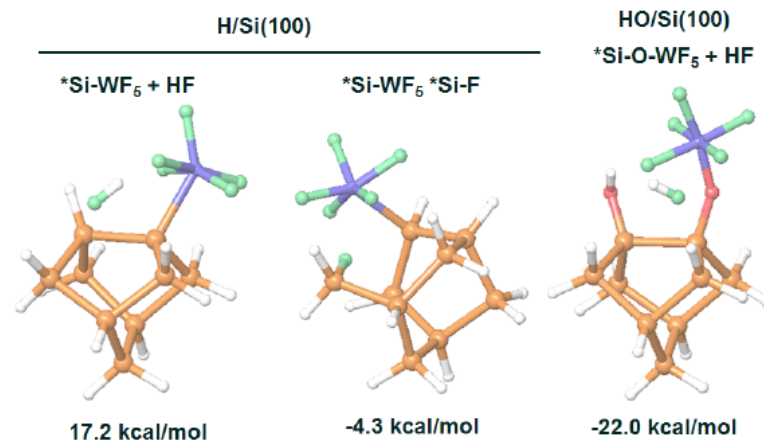


Figure 2. M06-DFT optimized surface products for interaction of a reference reaction using WF_6 with H/Si or HO/Si surface sites. Si atoms are in yellow, H in white, F in green, O in red and W in purple. WF_6 reactions with HO/Si sites are strongly favored.

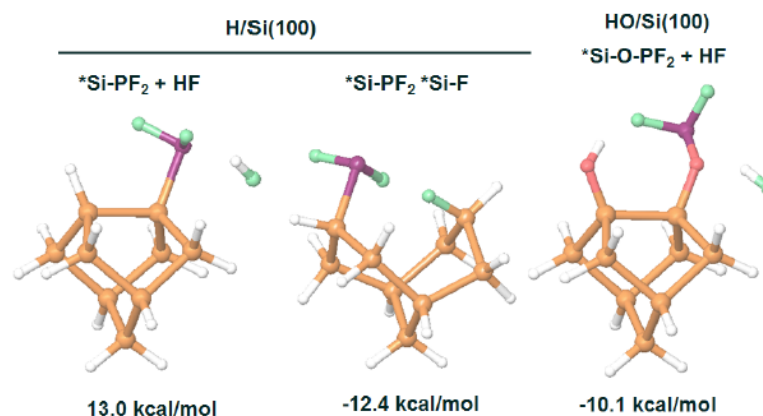


Figure 3. M06-DFT optimized surface products for interaction of PF_3 with H/Si or HO/Si surface sites. PF_3 reactions are favorable on both H/Si and HO/Si sites.

Density Functional Theory for B & P on Si (2)

More detailed DFT calculations show favorable enthalpies for PF_3 , PCl_3 and PBr_3 combined with Si_2H_6 .

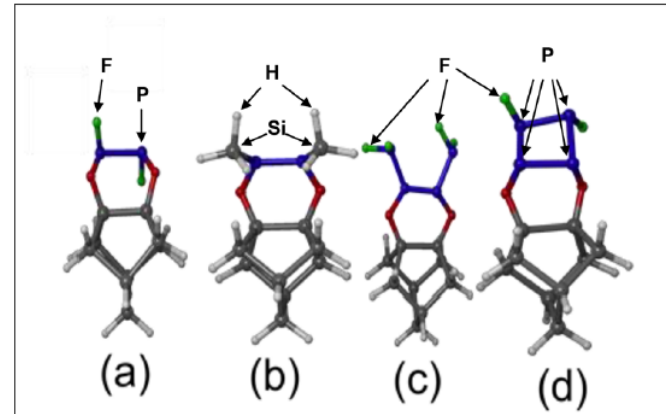


FIG. 4. (Color online) Phosphorus growth reactions. Reading from left to right, (a) shows a lateral bonded FP-PF configuration, (b) shows Si-H₃ terminations, (c) shows F terminations on the third and fourth P atoms, and (d) shows a (second) lateral bonding for the third and fourth P atoms in the growth stage.

TABLE I. Enthalpies for PF_3 , PCl_3 , and PBr_3 with Si_2H_6 (units are kcal/mol).

Chemistries →	$\text{PF}_3/\text{Si}_2\text{H}_6$	$\text{PCl}_3/\text{Si}_2\text{H}_6$	$\text{PBr}_3/\text{Si}_2\text{H}_6$
Process steps (below)			
First, second P nucleation	-4.7, -9.0	-20.0, -7.8	-22.4, -18.8
First lateral P-P bonding	-27.8	-20.8	-15.5
First, second F replacements	-21.9, -23.0	-19.3, -13.0	-16.4, -10.1
Third, fourth P growth	-13.4, -4.5	-17.0, -20.4	-18.6, -35.1
Second lateral P-P bonding	-37.7	-28.0	-22.1

T. Seidel, et al., "Simulation of nucleation and growth of ALD Phosphorous for doping of finFETs". JVST-A36 (2016).

Density Functional Theory for B & P on Si (3)

DFT calculations showed more favorable enthalpies for $B_2F_4^*$ for sequential depositions (for H-terminated Si surface) than BF_3 .

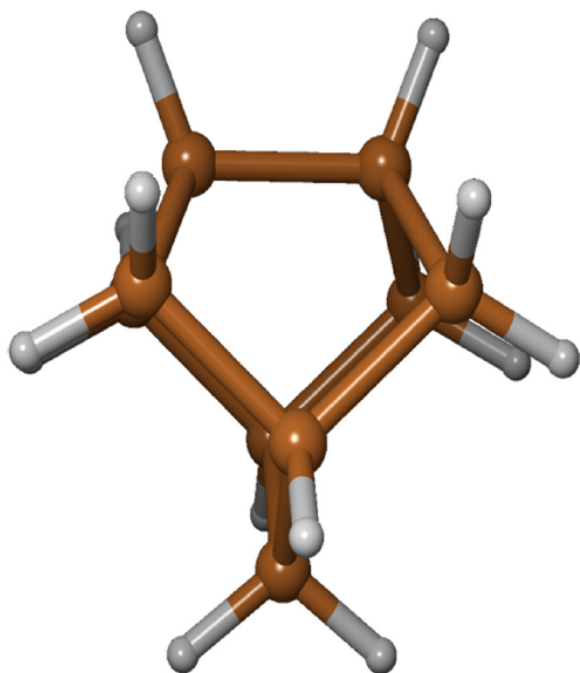


FIG. 1. (Color online) Model of a two-surface-atom Si(100) surface cluster (large spheres: Si, small spheres: H).

TABLE I. Nucleation enthalpies for BF_3 and B_2F_4 reactions.

Nucleation enthalpies	BF_3 (kcal/mol)	B_2F_4 (kcal/mol)
Si-H 1st reaction	28	-6.9
Si-H 2nd reaction	42	-15
Si-OH 1st reaction	-12	-41
Si-OH 2nd reaction	3.2	-22

* B_2F_4 is a relatively new Si process chemical with lower ionization potential than BF_3 (good for ion implant sources). Also weak B-B bonds.

A. Mane et al., "ALD of Boron-containing films using B_2F_4 ", JVST-A43 (2016).

ALD Growth Kinetics of B on Si (1)

Working on B-doped ALD, sequences of B_2F_4 alternated with H_2O showed eventual film growth saturation.

Sequences of B_2F_4 alternated with Si_2H_6 showed even sooner film growth saturation.

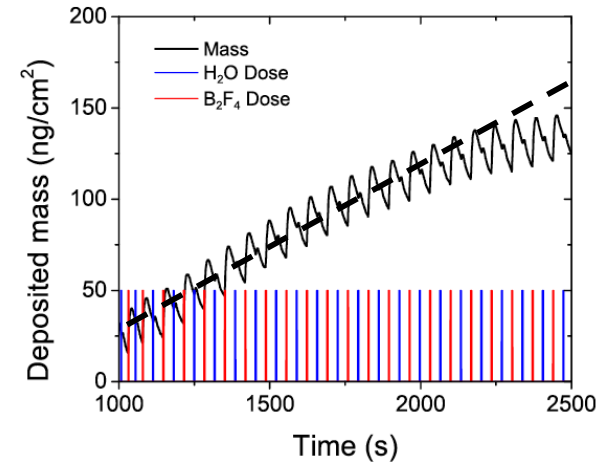


FIG. 2. (Color online) QCM mass uptake (top trace) versus time, and precursor dosing periods using alternating B_2F_4 and H_2O exposures at $300^\circ C$ using the timing sequence (4-20-4-20).

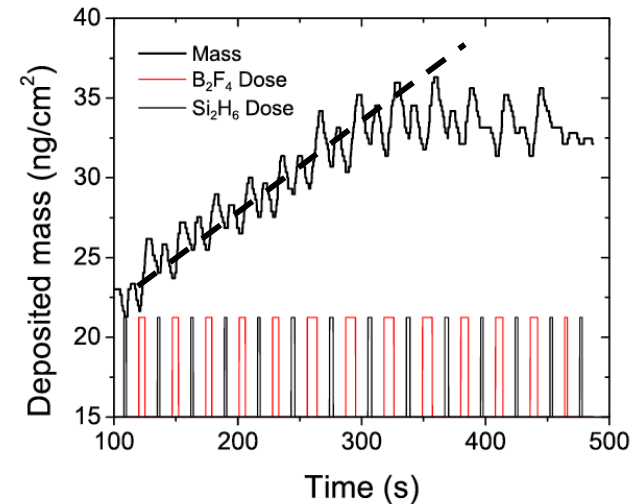


FIG. 3. (Color online) QCM mass uptake (top trace) versus time, and precursor dosing periods using alternating B_2F_4 and Si_2H_6 exposures at $300^\circ C$ using the timing sequence (5-10-2-10).

A. Mane et al., "ALD of Boron-containing films using B_2F_4 ", JVST-A43 (2016).

ALD Growth Kinetics of B on Si (2)

Sequences of B_2F_4 alternated with Si_2H_6 and H_2O also showed film growth saturation within ≈ 300 s.

But addition of TMA (Trimethyl-Al) to sequences of B_2F_4 alternated with H_2O showed continued film growth promise.

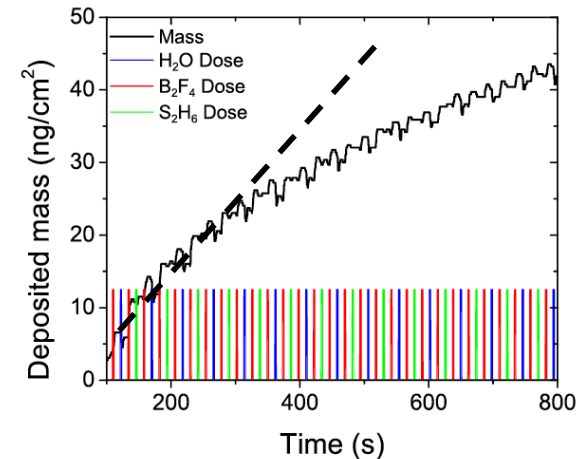


Fig. 4. (Color online) QCM mass uptake (top trace) versus time, and precursor dosing periods using the precursor sequence: B_2F_4 - H_2O - B_2F_4 - Si_2H_6 at $300^\circ C$ using 2 s dose and 10 s purge for each precursor.

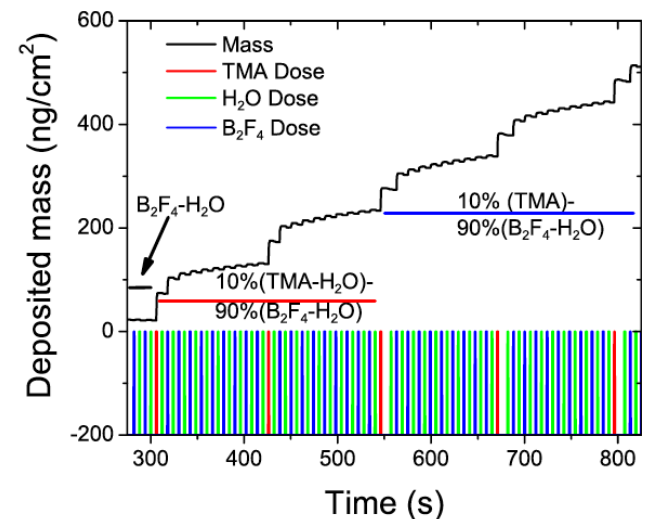


Fig. 5. (Color online) QCM mass uptake initiation with B_2F_4 - H_2O cycles followed by 10% (TMA- H_2O)/ 90% (B_2F_4 - H_2O), and 10% (TMA)/ 90% (B_2F_4 - H_2O) precursor sequences at $300^\circ C$ using 1 s dose and 10 s purge for each precursor.

A. Mane et al., "ALD of Boron-containing films using B_2F_4 ", JVST-A43 (2016).

ALD Growth Kinetics of B on Si (3)

A sequence of B_2F_4 alternated with TMA and H_2O showed linear film growth with no saturation.

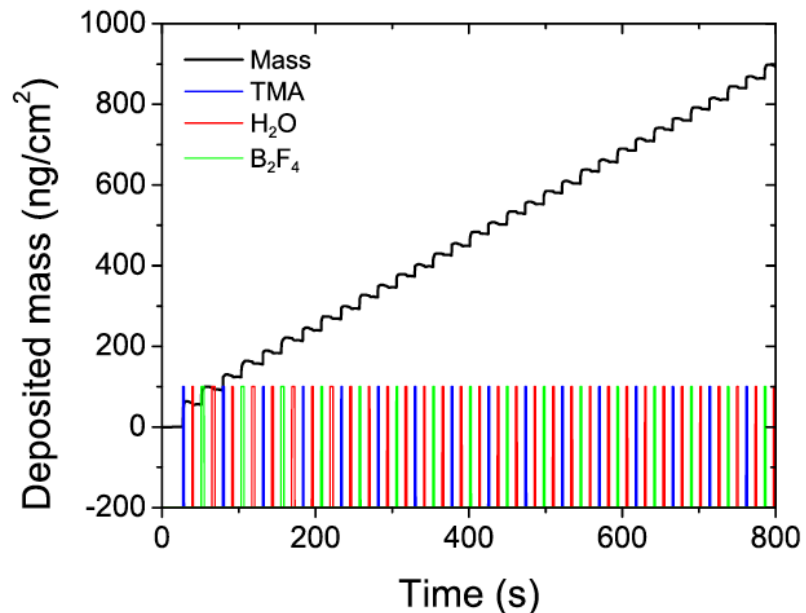


FIG. 6. (Color online) QCM mass uptake (top trace) versus time, and precursor dosing periods using the precursor sequence: B_2F_4 - H_2O -TMA- H_2O at $300^\circ C$ with 2 s dose and 10 s purge for each precursor to deposit a 50% $B_xAl_{2-x}O_3$ composite film.

However...

The resulting film is not really “dopant rich”, with $\approx 10\%$ B.

TABLE II. XPS composition (at. %) for B_2F_4 - H_2O -TMA- H_2O ALD films.

		Element			
Al	O	B	C	F	
39.9	36.6	9.3	6.9	7.1	

A. Mane et al., “ALD of Boron-containing films using B_2F_4 ”, JVST-A43 (2016).

B-rich Films with B_2F_4 : Conformality

Bottom of a 40:1
hollow Si cylinder*

B-AlBO thermal ALD films
showed excellent conformality
on the outside and inside of a
40:1 hollow Si cylinder.

Si core (8 nm)
B-AlBO (9 nm)
ZnO cap (6 nm)

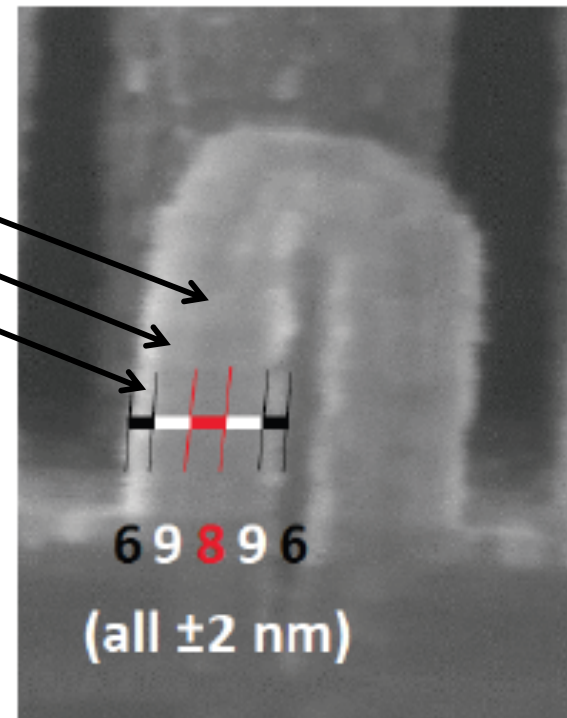


Fig. 4. SEM of conformal 9 nm B-AlBO ALD (with a 6 nm ZnO cap) at bottom of an 8 nm 40:1 aspect ratio cylinder.

* Aixtron test structure.

B-rich Films with B_2F_4 : Thermal Drive-in

“RTA” (30 s) annealing of B-AIBO ALD films produced ≈ 5 nm Xj profiles in Si for temperatures of 700 to 875 C.

F was the only significant co-diffuser with B from the B-AIBO ALD films at 825 C.

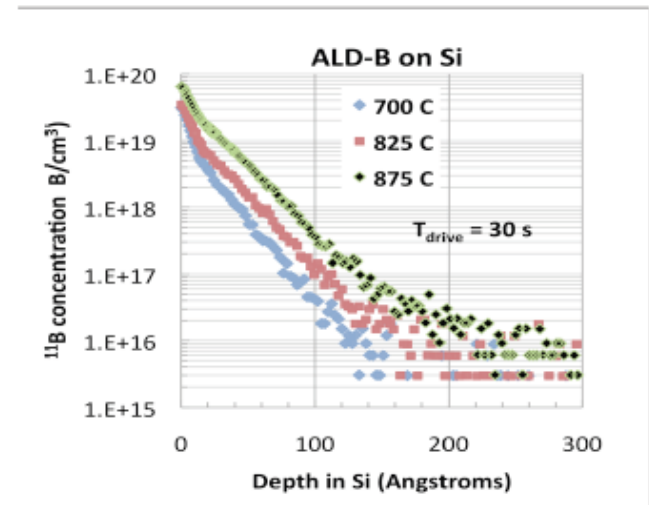


Fig. 6 PCOR SIMS ^{11}B profiles after RTA drive-ins at different temperatures from 8 nm thick B-doped AIBO ALD films.

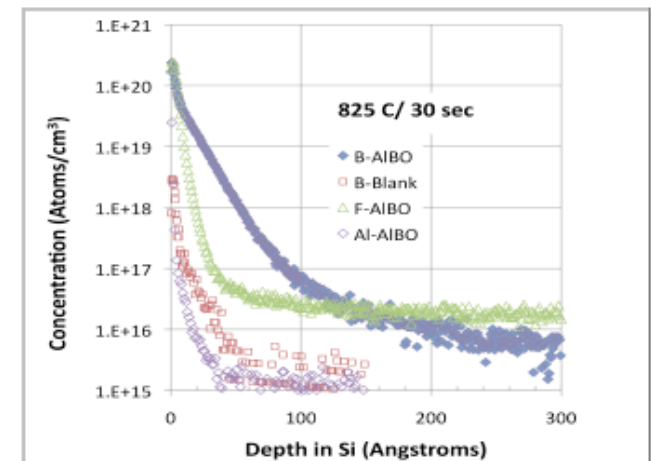


Fig. 5. ^{11}B PCOR SIMS profiles from a 200Å AIBO film after RTA 825°C/ 30 sec. $C_{surface} \approx 1E20$ B/cm³, and integrated boron content is 1.4E14 B/cm². The ^{11}B profile from a “blank” Si sample control. $C_{surface} \approx 1E18$ B/cm³, and integrated boron content is 1.1E11 B/cm². Also shown are F and Al diffused from the AIBO sample (with similar profiles as from the unprocessed blank Si control).

Summary & Status

1. Starting from an open field in late 2014, promising dopant rich film growth energetics identified for B and P containing films with DFT by Schrodinger Inc.
2. Growth kinetics of B-rich films explored by ANL for B_2F_4 , with linear growth conditions established.
3. B-containing thermal ALD films grown with excellent conformality and successful thermal drive in.
4. Papers written for ALD and IIT conferences.
5. Project on hold, pending arrival a serious sponsor (with funding) and ambitions to exploit these thermal ALD possibilities.

Acknowledgements

ACKNOWLEDGMENTS

We acknowledge Steve Shatas of Modular Process Technology and UCSD for thermal annealing, Jeff Mayer and John Marino of EAG for SIMS analysis, Entegris/ATMI for B₂F₄ materials, Aixtron Silicon Group for the high aspect ratio test structure and Alexander Goldberg and Matt Halls of Schrodinger for DFT calculations.

The cartoon I pasted into my 1st Silicon Valley notebook in 1980

But, getting ideas is the easy part.....

Notes for modern
(2015) graduate
students at Cheng
Kung U. (Tianan), who
never have seen a
typewriter.

Typewriter:
An archaic device,
before keyboards,
that printed directly
on **paper**.



*"Getting the ideas is the easy part....
the hard part is hitting one key at a time"*